

Modelling of vortex induced vibration for two degrees of freedom

Manish .A. Dhanwani*, Abhijit Sarkar†and B.S.V. Patnaik‡

* ‡ *Fluid Mechanics Laboratory, Department of Applied Mechanics.*

† *Machine Design Laboratory, Department of Mechanical Engineering.
Indian Institute of Technology Madras, Chennai 600036, India.*

ABSTRACT

The vortex-induced vibrations of an elastically mounted rigid cylinder free to move in-line and transverse to the flow are modelled through a lower order model. A simplified lumped mass model is proposed to model the two degree of freedom(d.o.f) structural oscillator. A classical Vander Pol equation along with acceleration coupling models the near wake dynamics describing the fluctuating nature of vortex shedding. The model dynamics is investigated analytically and the results are compared for moderate mass ratios. The results predicted using this model show a good agreement with the experimental data. The dependence of stream-wise displacement on mass and damping is explored. The cause of cross-flow displacement magnification attributed to oscillations in stream-wise direction is explored using the proposed model.

1. INTRODUCTION

VIV (Vortex Induced Vibrations) are a well known phenomenon to engineers as they occur in many situations such as: offshore structures and structures subject to wind loads such as pipes, risers, mooring lines, chimneys, suspended cables for bridges, power transmission lines etc. The practical significance of VIV has led to a large number of fundamental studies. Vortex induced vibrations(VIV) may lead to degradation of structural performance or possibly even structural failure. Several ways have been adopted to predict the dynamic behaviour of structures experiencing VIV.

One VIV prediction method consists of solving the Navier-Stokes equations by the Direct Numerical Simulation (DNS) for the fluid around the circular cylinder and to compute the

*Corresponding author, Research Scholar, Email: manish.dhanwani1988@gmail.com

†Assistant Professor, Email: asarkar@iitm.ac.in

‡Associate Professor, Email: bsvp@iitm.ac.in

hydrodynamic loads on it as presented by Newmand (1997) and Yong (2008). However, this approach is made difficult by the fact that Reynolds numbers in most industrial applications cannot be well estimated. Another well known method to predict VIV is by the force-decomposition model as reported in Blevins (2001) and Ogink (2010). In this technique, the measured fluid forces are directly used as forcing terms in the equation of structural motion. These fluid forces are measured by forced vibration experiments. The measured fluid force is then decomposed in two parts, a part which is in phase with the cylinder acceleration acts as added mass, and a part in phase with the cylinder velocity acts as added damping. The advantage of the force-decomposition method is that one can measure the fluid forces for specific cases, such as for a certain Reynolds number or for a certain cylinder roughness and then apply the measured forces in a direct manner. The disadvantage of this method is however that for long flexible cylindrical structures the response due to vortex shedding contains contribution from several waves. It is unlikely that a vibratory pattern containing multiple frequencies can be predicted accurately by using fluid forces that have been measured at a single frequency.

A well-known alternative is to use phenomenological models based on wake oscillators. Combined with accessible analytical considerations, they help in revealing the underlying physical nature. In this method instead of direct application of measured fluid forces to the equation of structure, wake oscillator models the cross-flow fluid force. The structural oscillator is combined to the wake oscillator by a suitable coupling (Hartlen and Currie 1970, Skop and Balasubramanian 1997). In most cases an equation of the Vander Pol or Rayleigh type is used, as these equations predict a limit cycle in the phase space. Facchinetti *et al.* (2004) presented an excellent review on the dynamics of wake oscillator models for vortex induced vibrations. Three different types of coupling effects (displacement, velocity and acceleration) of the cylinder movement on the lift fluctuation were considered. The advantage of the phenomenological models compared to the force decomposition method is that there is no assumption of a single dominant frequency of motion. The model finds the frequency, amplitude of the cylinder motion and the cross-flow fluid force on it's own. The disadvantages of the wake oscillator model is that there are no direct methods to derive the non-linearity parameter and the coupling term. Therefore, all wake oscillator models contain tuning parameters to adjust the model to the results of experiments.

Although the phenomenon of VIV of bluff bodies has been studied extensively, the vast majority of these studies have concentrated solely on transverse vibrations. Although the lift fluctuation is generally quite larger than the drag fluctuation, the resultant stream wise vibration must have some effect upon the wake and the response. Previous studies that have looked at 2-d.o.f mechanical systems have indicated that while the behaviour is qualitatively similar, some interesting differences exist. The transverse direction amplitude experiences a jump if the cylinder is free to vibrate in in-line direction as compared to the case in which in-line motion is restricted. Also the lock-in region was reported to be observed for a larger range of velocity by Moe *et al.* (1990). However, Jauvtis and Williamson (2008) reported that the freedom to oscillate in-line direction has a very little affect on the transverse vibrations for

high mass ratios. The same response branches, peak amplitudes, and vortex wake modes were reported to be found for both Y(transverse)-only and X(in-line), Y(transverse) motion. However, a dramatic change in the fluid structure interactions was observed when mass ratios were reduced below 6.

Recent reviews on the VIV can be found in (Sarpkaya 2004, Williamson and Govardhan 2008 and Gabbai and Benaroya 2005). Considering these characteristics of 2 d.o.f VIV, there is definitely a need to have a critical analysis in terms of the fundamental behaviour associated with the simplest forms of the model. In the present work, the above mentioned observations for VIV of 2 d.o.f structures are attempted by a simple mathematical model and various other features are investigated. An uncoupled structural oscillator is used to model the cylinder motions in in-line and transverse directions where as the Vander Pol oscillator is used to model the fluid forces in both in-line and transverse directions. In order to keep the model as simple as possible, only linear coupling terms for the fluid structure interactions are considered. The model dynamics is investigated analytically using acceleration coupling. The values of all model parameters have been tuned to match the experimental results for moderate mass ratios using the results reported by Jauvtis and Williamson (2008) as reference.

2. STRUCTURAL OSCILLATOR

A simplified model for a circular cylinder free to vibrate in in-line as well as transverse direction is presented. Fig. 1 shows the schematic of the model and the model parameters are given in Table 1.

Parameters	Description	Parameters	Description
m_s	Mass of the cylinder	U_0	Free stream velocity
k_1 & k_2	Support stiffnesses	c_1 & c_2	Damping
x	In-line/Stream-wise direction	y	Transverse/Cross-flow direction

Table 1: Description of the model parameters.

The force balance equations in transverse and in-line direction of flow are

$$m_s \ddot{x} + k_2 x + c_2 \dot{x} = F_x, \quad m_s \ddot{y} + k_1 y + c_1 \dot{y} = F_y \quad (1)$$

Here the mass, fluid forcing, damping and stiffness parameters are defined per unit length. The fluid forcing F_x and F_y due to the fluid near wake on the structure which is due to vortex shedding and fluid added mass is given as

$$F_x = \rho U_0^2 DC_{vx}/2 - m_a \ddot{x}, \quad F_y = \rho U_0^2 DC_{vy}/2 - m_a \ddot{y} \quad (2)$$

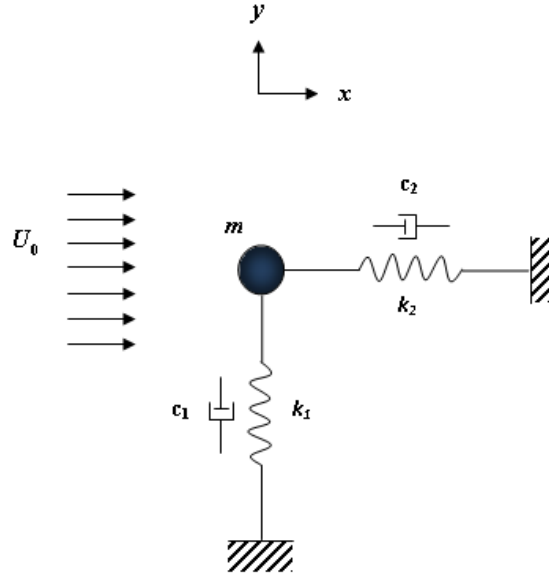


Fig. 1: Schematic of the present model

where ρ is the density of the fluid, D is the diameter of the cylinder, m_a is the fluid added mass, C_{vy} is the cross-flow vortex force coefficient and C_{vx} in-line vortex force coefficient (Blevins 2001). The fluid-added mass m_a which models inviscid inertial effects is given as $m_a = C_M \rho \pi D^2 / 4$, where C_M is the added mass coefficient. For a circular cylinder the value of added mass coefficient is taken to be unity (Blevins 2001).

The fluid forces on the structure are a function of relative velocities between the fluid and structure. The vortex force coefficients in terms of vortex lift coefficient (C_{VL}) and vortex drag coefficient (C_{VD}) as seen from Fig. 2 can be given as (Ogink *et al.* 2010)

$$C_{Vy} = (C_{VD} \sin \lambda + C_{VL} \cos \lambda) \frac{U^2}{U_0^2}, \quad C_{Vx} = (C_{VD} \cos \lambda - C_{VL} \sin \lambda) \frac{U^2}{U_0^2} \quad (3)$$

where the total velocity U and flow angle λ are

$$U = \sqrt{(U_0 - \dot{x})^2 + \dot{y}^2} \approx \sqrt{U_0^2 - 2U_0\dot{x}} \quad \text{and} \quad \lambda = \tan^{-1} \left(\frac{-\dot{y}}{U_0 - \dot{x}} \right) \quad (4)$$

Assuming the cylinder velocity to be very small as compared to the free stream velocity ($\dot{y} \ll U_0$ and $\dot{x} \ll U_0$), from Eq. (4), we get $\sin \lambda = \frac{-\dot{y}}{U_0}$, $\cos \lambda = 1$. Substituting these approximations for $\sin \lambda$ and $\cos \lambda$ in Eq. (3), the force coefficients in transverse and in-line direction can be given as

$$C_{Vy} = C_{VL} - \frac{\dot{y}}{U_0} C_{VD} - \frac{2\dot{x}}{U_0} C_{VL}; \quad C_{Vx} = C_{VD} + \frac{\dot{y}}{U_0} C_{VL} - \frac{2\dot{x}}{U_0} C_{VD}. \quad (5)$$

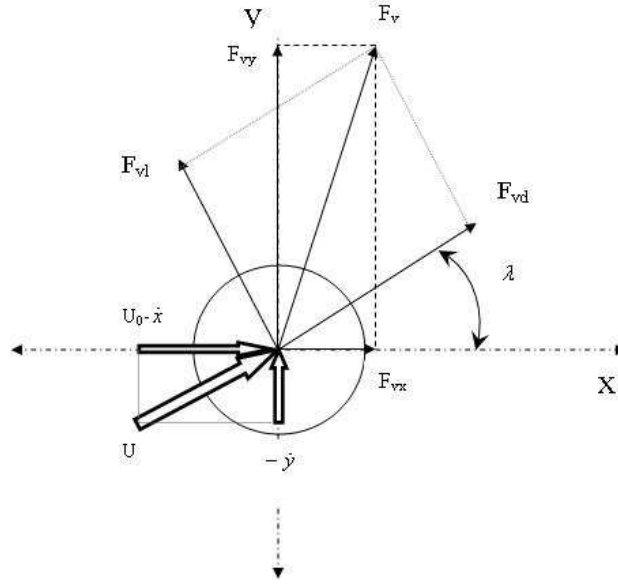


Fig. 2: Schematic showing the decomposition of the vortex fluid force along the horizontal and vertical directions.

From Eqs. (1), (2) and (5), the governing equation in stream-wise and cross-flow directions can be given as

$$(m_s + m_a)\ddot{x} + k_2x + \left(c_2 + \frac{2\rho U_0 DC_{VD}}{2}\right)\dot{x} - \frac{\rho U_0 DC_{VL}}{2}\dot{y} = \frac{\rho U_0^2 DC_{VD}}{2} \quad (6)$$

$$(m_s + m_a)\ddot{y} + k_1y + \frac{\rho U_0 DC_{VL}}{2}\dot{x} + \left(c_1 + \frac{\rho U_0 DC_{VD}}{2}\right)\dot{y} = \frac{\rho U_0^2 DC_{VL}}{2} \quad (7)$$

In the above equations the terms $(\rho U_0 DC_{VD}/2)$ and $(\rho U_0 DC_{VL}/2)$ account for the fluid-added damping. C_{VD} and C_{VL} are periodic functions of time and their periodicity will be determined in section 5. Among the studies concentrating on the XY motion of the cylinder, some of them were carried out for different mass ratios in in-line and transverse directions (Moe *et al.* 1990) whereas some had the same mass ratios for both the directions (Jauvtis and Williamson 2008, Sanchis *et al.* 2008). In this analysis, the mass is considered to be same for both the directions.

Non dimensionalizing the dependent variables (*viz.* x and y) and independent variable t in Eqs. (6) and (7) as

$$X = x/D, \quad Y = y/D \quad \text{and} \quad T = t\Omega_f$$

where Strouhal frequency $\Omega_f = 2\pi StU_0/D$. Thus the non-dimensional equations of structural oscillator in in-line and transverse direction are given as

$$Y'' + \left(2\zeta_1\delta_1 + \frac{\gamma}{\mu}\right) Y' + \left(\frac{2\chi}{\mu}\right) X' + \delta_1^2 Y = \frac{C_{VL}}{8\pi^2 St^2 \mu} \quad (8)$$

$$X'' + \left(2\zeta_2\delta_2 + \frac{2\gamma}{\mu}\right) X' - \left(\frac{\chi}{\mu}\right) Y' + \delta_2^2 X = \frac{C_{VD}}{8\pi^2 St^2 \mu} \quad (9)$$

where (') indicates the derivative with respect to non-dimensionalized time T , ζ_1 and ζ_2 are the damping ratios and other non-dimensional parameters (*viz.* δ_1 , δ_2 , μ , γ and χ) are enlisted below.

$\delta_1 = \Omega_{s1}/\Omega_f = \Omega_{s1}/(2\pi StU/D)$	$\delta_2 = \Omega_{s2}/\Omega_f = \Omega_{s2}/(2\pi StU/D)$
$\Omega_{s1} = \sqrt{\frac{k_1}{m}}$	$\Omega_{s2} = \sqrt{\frac{k_2}{m}}$
$m = m_s + m_a$	$\mu = m/\rho D^2$
$\gamma = C_{VD}/4\pi St$	$\chi = C_{VL}/4\pi St$

In this case the stiffnesses in stream-wise and cross-flow directions are considered to be the same ($\Omega_{s1} = \Omega_{s2} = \Omega_s$). Thus

$$\delta_1 = \delta_2 = \frac{1}{StU_r} \quad \text{where reduced velocity } U_r = 2\pi U/\Omega_s D.$$

The drag coefficient C_{VD} depending on the structure's transverse motion can be written as $(1 + 2Y_0)C_{VD0}$ (Blevins 2001), where C_{VD0} is the drag coefficient for stationary cylinders. The value of C_{VD0} in the sub-critical Reynolds number regime $300 < Re < 1.5 \times 10^5$, is given as $C_{VD0} = 1.2$ (Facchinetti 2004). The value of lift coefficient C_{VL0} for a stationary cylinder in the sub-critical regime is taken to be 0.3 (Facchinetti 2004). For the sake of simplicity we assume here a constant amplified drag coefficient $C_{VD} = 2$ (Facchinetti 2004) and a constant lift coefficient $C_{VL} = 0.5$ and hence $\gamma = 0.8$ and $\chi = 0.2$. Now, the equations governing the structural motion in stream-wise (Eq. 8) and cross-flow (Eq. 9) direction become constant coefficient ordinary differential equations. Also the value of Strouhal number in the sub-critical Reynolds number regime is taken to be 0.2 (Blevins 2001).

3. WAKE OSCILLATOR

In the present work the fluctuating nature of the vortex street is modelled as a Vander Pol oscillator. The wake oscillator equations in in-line and transverse directions are given as

$$\ddot{q} + \epsilon\Omega_{fy}(q^2 - 1)\dot{q} + \Omega_{fy}^2 q = S_y,$$

$$\ddot{p} + \psi\Omega_{fx}(p^2 - 1)\dot{p} + \Omega_{fx}^2 p = S_x.$$

The dimensionless wake variables q and p are associated to the fluctuating lift coefficient and fluctuating drag coefficient as $C_{VL} = qC_{VL0}/2$ (Facchinetti 2004) and $C_{VD} = pC_{VD0}/2 + p/\delta_1$ (Kim and Perkins 2002), where the reference lift coefficient C_{VL0} and reference drag coefficient C_{VD0} are that observed on a fixed structure subjected to vortex shedding, Ω_f is the Strouhal frequency, Ω_{fx} is the vortex shedding frequency in in-line direction and Ω_{fy} is the vortex shedding frequency in cross-flow direction. The fluid variables q and p are referred as a reduced vortex lift coefficient and reduced vortex drag coefficient respectively. As reported by Jauvtis and Williamson (2008), the cause of stream-wise vibrations is that, as each vortex is shed, a fluctuating drag is generated, so that the forcing frequency is twice that for the transverse direction.

$$\Omega_{fx} = 2\Omega_{fy} = 2\Omega_f.$$

The right hand side forcing terms S_x and S_y model the effects of the cylinder motion on the near wake. These force may either be proportional to the displacement of the cylinder (displacement coupling) or velocity of the cylinder (velocity coupling) or acceleration of the cylinder (acceleration coupling). The results corresponding to the acceleration coupling showed good agreement with the experimental results for the model proposed by Facchinetti *et al.* (2004). As the present model is an extension of the model proposed by Facchinetti *et al.* (2004), acceleration coupling has been used to model the effect of cylinder motion on the near wake for both stream-wise and cross-flow directions. Hence, the wake oscillator equations in stream-wise and cross-flow directions can be given as

$$\ddot{q} + \epsilon\Omega_{fy}(q^2 - 1)\dot{q} + \Omega_{fy}^2 q = a\ddot{Y}$$

$$\ddot{p} + \psi\Omega_{fx}(p^2 - 1)\dot{p} + \Omega_{fx}^2 p = b\ddot{X}.$$

Non-dimensionalization results in,

$$q'' + \epsilon(q^2 - 1)q' + q = AY'' \quad (10)$$

$$p'' + 2\psi(p^2 - 1)p' + 4p = BX'' \quad (11)$$

Here, A , ϵ , B and ψ are the parameters whose values are to be determined based on mass and damping in order to fit the experimental data.

4. GOVERNING EQUATIONS & MODEL PARAMETERS

The equations governing the structural motion (Eq. 8 and Eq. 9) can be written in terms of reduced vortex lift coefficient q and reduced vortex drag coefficient p

$$Y'' + \left(2\zeta_1\delta_1 + \frac{\gamma}{\mu}\right) Y' + \left(\frac{2\chi}{\mu}\right) X' + \delta_1^2 Y = Nq \quad (12)$$

$$X'' + \left(2\zeta_2\delta_2 + \frac{2\gamma}{\mu}\right) X' - \left(\frac{\chi}{\mu}\right) Y' + \delta_2^2 X = Mp \quad (13)$$

where

$$M = \frac{C_{D0} + 1}{16\pi^2 St^2 \mu}, \quad N = \frac{C_{L0}}{16\pi^2 St^2 \mu}$$

Eq.(10),(11),(12) and (13) form the governing equations of the problem.

The mass ratio μ can directly be derived from the structure and fluid masses. The values of reference lift coefficient C_{VL0} and reference drag coefficient C_{VD0} are given to be equal to 0.3 and 1.2, respectively for a large Reynolds number regime (Blevins 2001). Hence, the values of M and N obtained from the above mentioned relations for $\mu = 6.9$ are 0.05 and 0.006 respectively. The mass, damping and stiffness are considered to be the same in transverse as well as in-line direction. Thus, $\zeta_1 = \zeta_2$ and $\delta_1 = \delta_2$. As this is a phenomenological model the values of the tuning parameters (*viz.* A , B , ϵ and ψ) have been found by comparing the stream-wise response X_0 given by the present model with the experimental data of Jauvitis and Williamson (2008). The experiments were reported to have been conducted at moderate mass and damping ($\mu = 6.9$ and $\zeta = 1.45 \times 10^{-3}$). Thus for moderate mass and damping, the values of wake oscillator parameters found by trial and error are $A = 5$, $\epsilon = 0.0035$, $B = 1$ and $\psi = 0.05$.

5. SOLUTION METHODOLOGY

Method of harmonic balancing is used to obtain the responses, frequency and phase differences. The responses of the structure (*viz.* X and Y) and the fluid forcing (*viz.* q and p) are considered to be harmonic in nature. As mentioned earlier, the frequency of fluctuating drag is twice that of fluctuating lift, thus

$$q = q_0 \cos(\omega t - \phi) \quad \text{and} \quad p = p_0 \cos(2\omega t - \beta).$$

The choice of X and Y motion is chosen to be

$$Y = Y_0 \cos(\omega t) \quad \text{and} \quad X = X_0 \cos(2\omega t - \alpha)$$

Substituting these in the Eq. (12), harmonic balancing leads us to

$$\tan \phi = -\frac{\omega(2\zeta\delta + \frac{\gamma}{\mu})}{\delta^2 - \omega^2}; \quad Y_0 = \frac{Nq_0}{\sqrt{(\delta^2 - \omega^2)^2 + \omega^2(2\zeta\delta + \frac{\gamma}{\mu})^2}}. \quad (14)$$

Performing harmonic balancing on Eq. (10) gives

$$q_0 = 2\sqrt{1 + \frac{AN\omega^2 + (1 - \omega^2)(\delta^2 - \omega^2)}{\epsilon\omega^2(2\zeta\delta + \frac{\gamma}{\mu})}} \quad (15)$$

and elementary algebra leads us to

$$\omega^6 - \omega^4(1 + 2\delta^2 - (2\zeta\delta + \frac{\gamma}{\mu})^2) - \omega^2(-2\delta^2 - \delta^4 + (2\zeta\delta + \frac{\gamma}{\mu})^2) - \delta^4 + AM\omega^2(\omega^2 - \delta^2) = 0. \quad (16)$$

Similarly harmonic balancing on Eq. (13) yields

$$\tan \beta = \frac{\delta^2 \sin \alpha - 4\omega^2 \sin \alpha - 2\omega(2\zeta\delta + \frac{2\gamma}{\mu}) \cos \alpha}{\delta^2 \cos \alpha - 4\omega^2 \cos \alpha + 2\omega(2\zeta\delta + \frac{2\gamma}{\mu}) \sin \alpha}; \quad X_0 = \frac{Mp_0}{\sqrt{E^2 + R^2}} \quad (17)$$

and harmonic balancing on (11) yields

$$p_0 = 2\sqrt{1 - \frac{1}{E\psi} \left(\frac{(1 - \omega^2)R}{\omega} + BM\omega \cos \alpha \right)} \quad (18)$$

$$\tan(\alpha) = \frac{(1 - \omega^2) \sin(\beta) + \omega \psi \left(1 - \frac{p_0^2}{4}\right) \cos(\beta)}{(1 - \omega^2) \cos(\beta) - \omega \psi \left(1 - \frac{p_0^2}{4}\right) \sin(\beta)} \quad (19)$$

where $E = \delta^2 \sin \alpha - 4\omega^2 \sin \alpha - 2\omega(2\zeta\delta + \frac{2\gamma}{\mu}) \cos \alpha$ & $R = \delta^2 \cos \alpha - 4\omega^2 \cos \alpha + 2\omega(2\zeta\delta + \frac{2\gamma}{\mu}) \sin \alpha$.

It has been verified that the residues of harmonic balancing are very small for high mass ratios ($\mu \gg 1$). Hence the results presented using this technique are inappropriate for low mass ratios.

6. DYNAMICAL BEHAVIOUR OF THE MODEL

The dynamical behaviour of the present system is analysed and its solutions are investigated for moderate mass ratio and damping. One of the principal interests in undertaking this research is to model the SS and AS modes of vortex shedding as reported by Williamson and Jauvtis (2008).

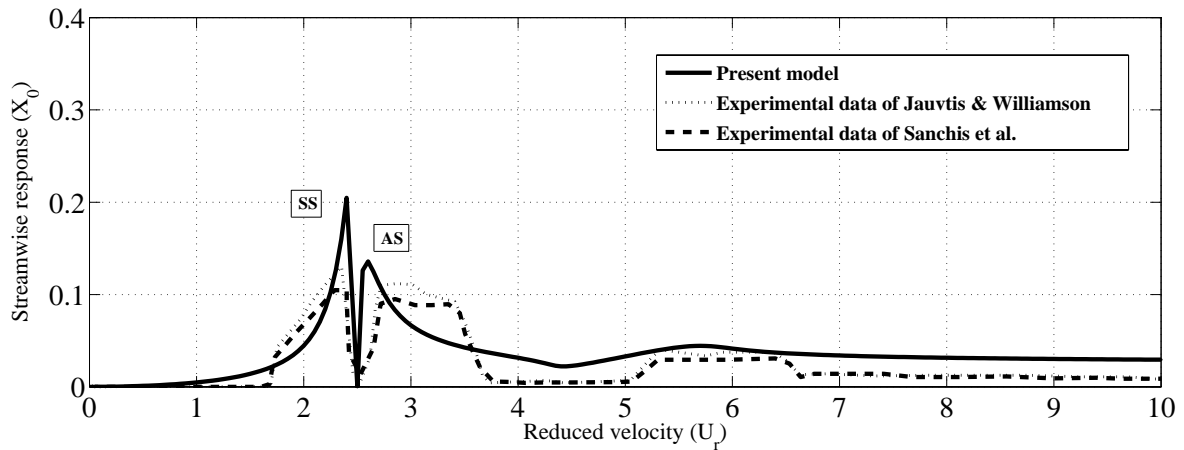


Fig. 3: Comparison of stream-wise response between the present model and the experimental data of Jauvtis and Williamson (2008) and Sanchis *et al.*(2008).

From Fig. 3 it is evident that the present model qualitatively predicts the SS and AS modes along with a slight jump in response at higher velocities $5 < U_r < 6.5$. As stated earlier the forcing frequency in stream-wise direction is twice that in cross-flow direction ($\Omega_{fx} = 2\Omega_{fy}$). It is known that the lift coefficient shows a fluctuation corresponding to cross-flow resonance(lock-in) at ($U_r \approx 5$)(Facchinetti *et al.* 2004). Hence, it is reasonable to expect fluctuations in drag for $U_r \approx 2.5$. These drag fluctuations are evident in Fig. 4.

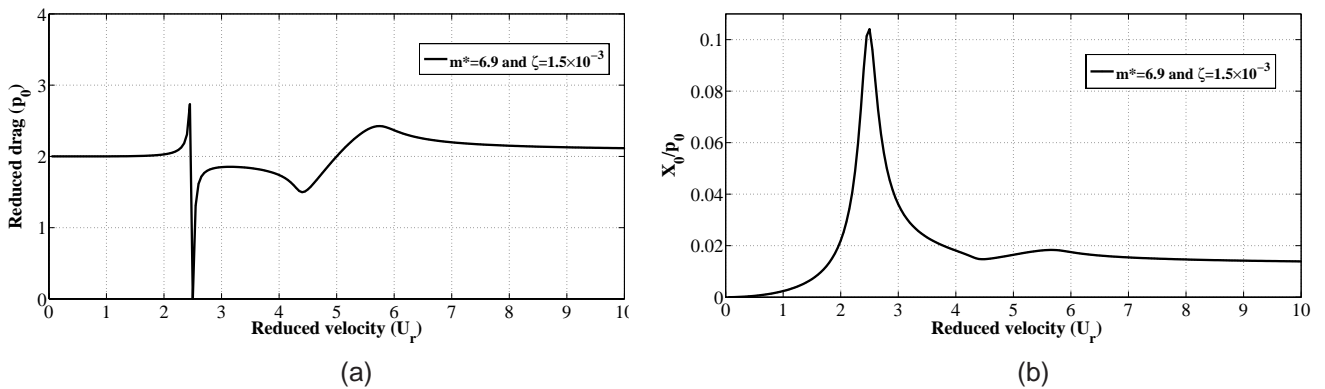


Fig. 4: (a) Plot demonstrating the behaviour of reduced drag p_0 with increasing velocity U_r . (b) Response of X_0/p_0 as a function of reduced velocity.

It is known that cross-flow resonance(lock-in) is observed at $U_r \approx 5$. Thus an increase in stream-wise amplitude is expected at $U_r \approx 2.5$, which corresponds to SS and AS branches

as reported by Jauvtis and Williamson (2008). But a sharp dip in amplitude at $U_r = 2.5$ is also observed separating the SS and AS modes. Thus in order to get a clear picture of the response characteristics in stream-wise direction, we plot X_0/p_0 (i.e. Output/Input) as a function of reduced velocity.

As observed from Fig. 4(b), the response peak of X_0/p_0 is symmetric about $U_r = 2.5$ which is a characteristic feature of linear resonance. Thus it can be inferred that the increase in stream-wise displacement amplitude at $U_r \approx 2.5$ corresponds to stream-wise resonance. The similarity between the stream-wise displacement response at $U_r \approx 2.5$ and resonance corresponding to linear theory is further brought out by the phase difference ($\alpha - \beta$) between X_0 and p_0 .

Linear theory predicts a phase shift of π across resonance as well as antiresonance. As observed from Fig. 5, there is an overall phase shift of π while crossing through the SS and AS modes of stream-wise response superimposed by another phase shift of π at $U_r = 2.5$. This is indicative of multi-scale phenomenon at $U_r = 2.5$. A similar overall phase shift of π while passing through cross-flow resonance(lock-in) was reported by Carberry *et al.*(2001) and is captured by the present model as shown in Fig. 5(b). In this context the SS and AS modes can be inferred as stream-wise resonance. The phase jump of π at $U_r \approx 5$ corresponds to an increase in reduced drag(p_0) across $U_r \approx 5$. Though VIV is a non-linear phenomenon, a few characteristics are analogous to the linear theory.

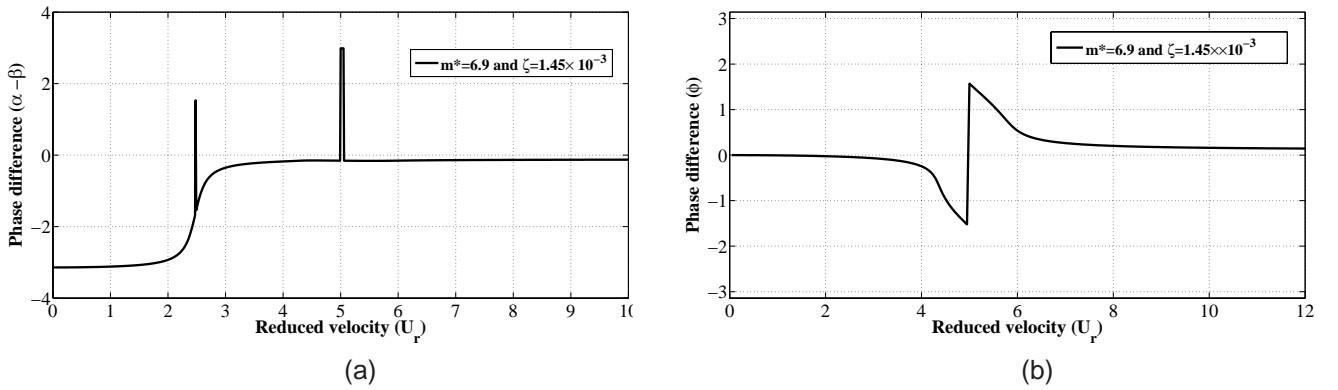


Fig. 5: (a) Variation of phase difference $\alpha - \beta$ between stream-wise displacement amplitude X_0 and reduced drag p_0 with reduced velocity U_r . (b) Variation of phase difference ϕ between transverse displacement amplitudes Y_0 and reduced lift q_0 with reduced velocity U_r .

According to the linear theory, the response at resonance is controlled only by damping. Calculations were carried out by varying the structural damping and a negligible change in response at resonance was observed. Thus, the reported response is not affected by structural damping but by the fluid in the form of Vander Pol oscillator which shows a limit

cycle behaviour.

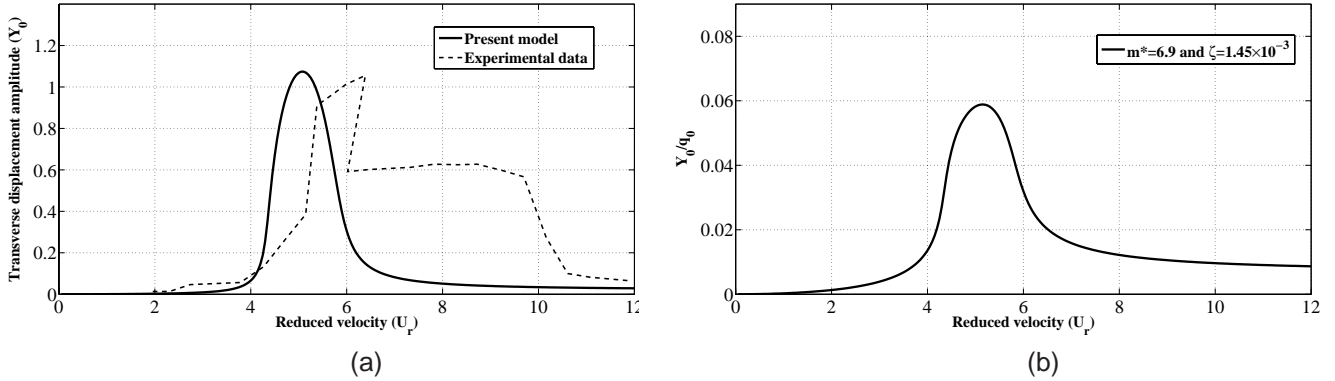


Fig. 6: Comparison between the present model and the experimental data of Jauvtis and Williamson (2008).

The comparison between the transverse response observed by Jauvtis and Williamson (2008) and that predicted by the present model is given in Fig. 6. As observed from Fig. 6, the magnitude of transverse response at resonance is predicted accurately. However, it occurs at a lower value of reduced velocity, with an under prediction of the width of the lock-in region. The response Y_0/q_0 predicts the cross-flow resonance at $U_r \approx 5$ in accordance with linear theory.

6.1. Effect of mass and damping on stream-wise displacement

As observed by Sanchis *et al.*(2008), the in-line displacement amplitude corresponding to the stream-wise resonance which occurs at low reduced velocities ($U_r \approx 2.5$) is almost the same for different mass ratios and damping whereas the in-line displacement amplitude corresponding to high reduced velocities ($U_r \approx 6.5$) varies on varying the mass ratio and damping. The experimental observations of Sanchis *et al.*(2008) demonstrating the above mentioned behaviour is given in Fig. 7 along with the corresponding response as predicted by the present model.

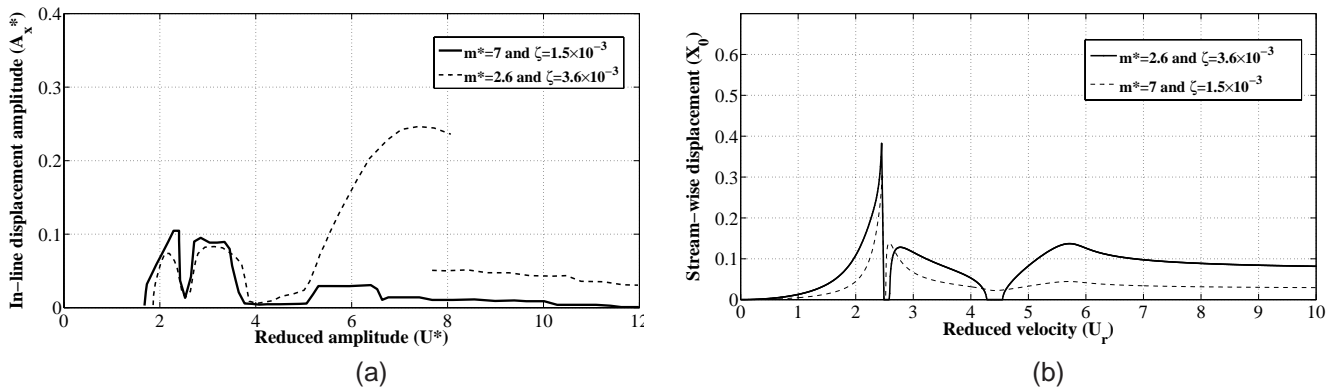


Fig. 7: (a) In-line displacement amplitude observed by Sanchis *et al*(2008) by varying mass ratios and damping simultaneously. (b) Corresponding response as predicted from the present model.

It is evident from Fig. 7 that the response predicted by present model qualitatively matches the experimental observations of Sanchis *et al*(2008). However, it is not clear which of the two parameters (*viz.* mass ratio or damping) is the cause of such a behaviour. Thus, in order to explore the parameter responsible for this behaviour in stream-wise amplitude, X_0 as a function of U_r is plotted by varying each parameter individually while keeping the other fixed.

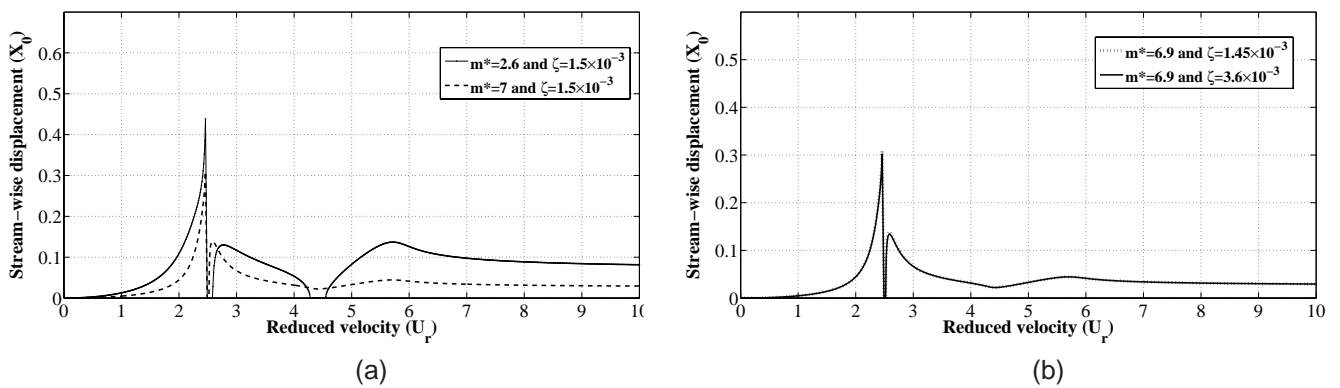


Fig. 8: (a) Effect of mass ratio on stream-wise displacement amplitude. (b) Effect of damping on stream-wise displacement amplitude.

Fig. 8 clearly brings out the dependence of stream-wise displacement on mass ratio while structural damping hardly has any effect on X_0 even at stream-wise resonance. This

independence on damping even at stream-wise resonance is due to the coupling of structural oscillator with the limit cycle(Vander Pol) oscillator. In the absence of this coupling, structural damping was seen to alter the response at stream-wise resonance.

6.2. Effect of stream-wise displacement on transverse displacement amplitude

In this section, the effect of freedom to move in stream-wise direction along with cross flow direction is explored. As in section 5, the choice of harmonic balancing technique to solve the governing equations led us to $\left(\frac{\dot{\chi}}{\mu} = 0\right)$ and hence uncoupled the equations governing the motion of structure. This also rendered the governing equations to be inaccurate for low mass ratios. In order to overcome these shortcomings, the governing equations have been solved numerically using the Runge-kutta solver. The governing equations solved are

$$Y'' + \left(2\zeta_1\delta_1 + \frac{\gamma}{\mu}\right) Y' + \left(\frac{2\chi}{\mu}\right) X' + \delta_1^2 Y = Nq \quad (20)$$

$$X'' + \left(2\zeta_2\delta_2 + \frac{2\gamma}{\mu}\right) X' - \left(\frac{\chi}{\mu}\right) Y' + \delta_2^2 X = Mp \quad (21)$$

$$q'' + \epsilon(q^2 - 1)q' + q = AY'' \quad (22)$$

$$p'' + 2\psi(p^2 - 1)p' + 4p = BX'' \quad (23)$$

The response as a function of reduced velocity for transverse only vibration(eq.20 and 22) and simultaneous stream-wise and transverse vibrations is plotted for low as well as high mass ratios.

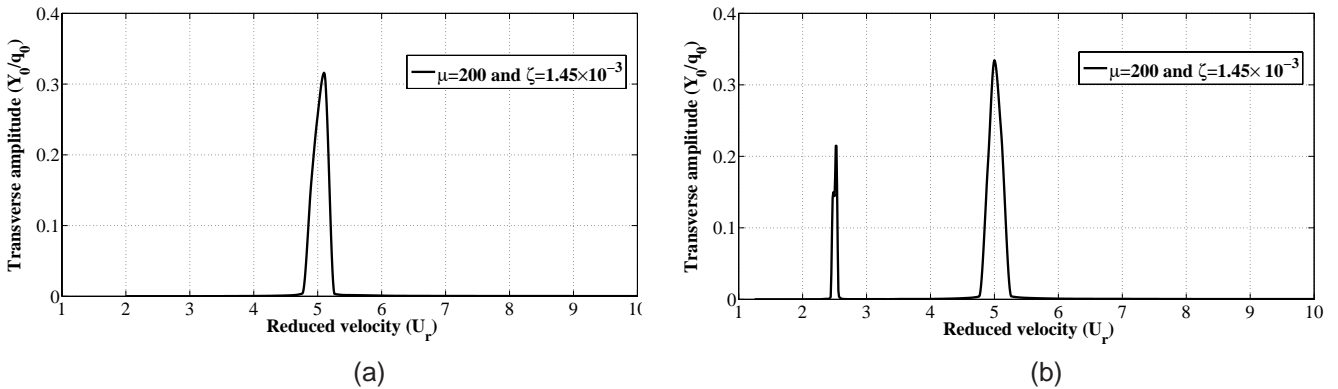


Fig. 9: Transverse displacement amplitude for high mass ratio($\mu = 200$) (a) transverse only vibration (b) stream-wise along with transverse vibration.

As observed from Fig. 9, for high mass ratios ($\mu = 200$) the cross-flow displacement amplitude $\left(\frac{Y_0}{q_0}\right)$ at cross-flow resonance is same for transverse only vibration (1 d.o.f) and stream-wise vibration along with transverse vibration (2 d.o.f). The velocity at which cross-flow resonance is observed is same for both the cases. This observation is in synchronization with the experimental observations as reported by Williamson and Jauvtis (2008) that for high mass ratio, the freedom to vibrate in stream-wise direction along with cross-flow direction does not affect the cross-flow response.

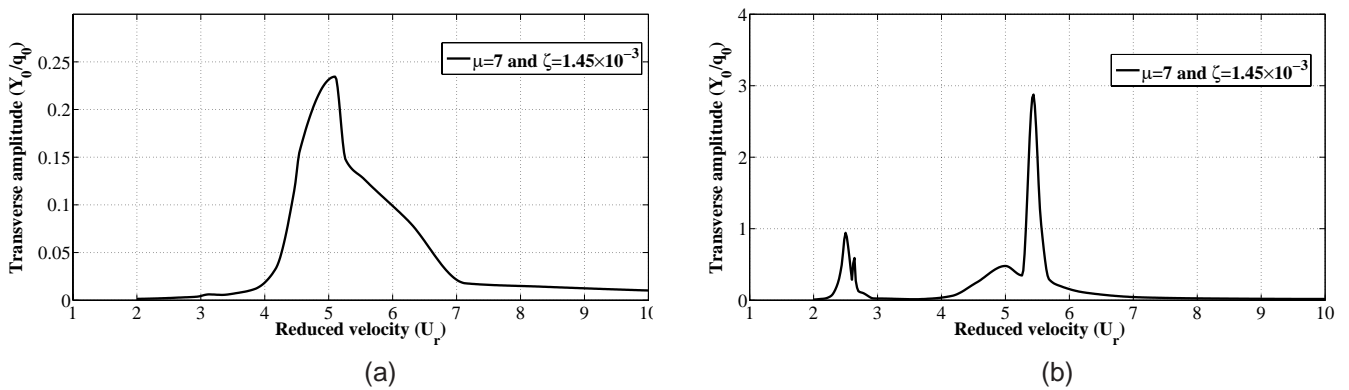


Fig. 10: Transverse displacement amplitude for low mass ratio ($\mu = 7$) (a) transverse only vibration (b) stream-wise along with transverse vibration.

As observed from Fig. (10), for low mass ratios ($\mu = 7$) the cross-flow displacement amplitude $\left(\frac{Y_0}{q_0}\right)$ shows a significant jump at cross-flow resonance for 2 d.o.f case as compared to 1 d.o.f case. Also the cross-flow resonance is observed at higher velocity for 2 d.o.f case as compared to 1 d.o.f case. These observations are in agreement with the experimental results reported by Williamson and Jauvtis (2008). Apart from this, a jump in cross-flow response at stream-wise resonance is observed for both low and high mass ratios corresponding to 2 d.o.f case.

7. SUMMARY & CONCLUSIONS

In the present study, uncoupled structural oscillators are used to model the structural dynamics. These structural oscillators in stream-wise and cross-flow direction are coupled with wake oscillator in respective directions through an acceleration coupling term. The oscillating mass and the natural frequency are same in both the directions. The ability of the model has been analysed by first estimating the values of all parameters by comparing with experimental data reported by Jauvtis and Williamson (2008). The equations were solved

using harmonic balancing technique for high mass ratios which uncouples the equations governing the motion of structure in stream-wise and cross-flow directions. These results have been systematically compared with experimental data. This model successfully models the stream-wise dynamics of VIV where as the cross-flow dynamics are rendered same as that for transverse only motion as the effect of stream-wise coupling is negligible for high mass ratios. It is observed that mass has significant effect on stream-wise displacement where as damping hardly effects X_0 . It is also concluded that, though VIV being a non-linear phenomenon shows certain characteristics analogues to linear theory. The existence of multi-scale phenomenon at stream-wise resonance was also observed. In order to bring out the effect of freedom to move in stream-wise direction, the governing equations were solved numerically using the Runge-kutta solver. The cause of jump in transverse displacement amplitude for XY motion as compared to Y only motion is found to be due to the additional fluid damping in stream-wise direction.

References

- [1] Blevins R.D. *Flow induced vibration* Second edition, Van Nostrand Reinhold, Krieger publishing company, Malabar, Florida.
- [2] Facchinetti M.L., Langre E.D, Biolley F. (2004), "Coupling of structure and wake oscillators in vortex-induced vibrations", *Journal of Fluids and Structures*, 19(2), 123-140,.
- [3] Gabbai R. D., Benaroya H. (2005), "An overview of modelling and experiments of vortex induced vibration of circular cylinders", *Journal of Sound and Vibration*, 282(3-5), 575-616.
- [4] Jauvtis, N., Williamson, C.H.K. (2004), "The effect of two degrees of freedom on vortex-induced vibration at low mass and damping", *Journal of Fluid Mechanics*, 509, 2362.
- [5] Khalak A. and Williamson C. H. K. (1999), "Motions, forces and mode transitions in vortex-induced vibrations at low mass-damping", *Journal of Fluids and Structures*, 13(7-8), 813-851.
- [6] Krenk S. and Nielsen S. R. K. (1999), "Energy balanced double oscillator model for vortex-induced vibrations", *ASCE Journal of Engineering Mechanics*, 125(3), 263-271.
- [7] Newmand D.J. and Karniadakis G.E. (1997), "A direct numerical simulation study of flow past a freely vibrating cable", *Journal of Fluid Mechanics*, 344(1), 95-136.
- [8] Ogink R.H.M. and Metrikine A.V. (2010), "A wake oscillator with frequency dependent coupling for the modelling of vortex-induced vibration", *Journal of Sound and Vibration*, 26(329), 54525473.

- [9] Sanchis A., Saelevik G. and Grue J. (2008), "Two-degree-of-freedom vortex-induced vibrations of a spring-mounted rigid cylinder with low mass ratio", *Journal of Fluids and Structures*, 24(6), 907-919.
- [10] Sarpkaya T. (2004), "A critical review of the intrinsic nature of vortex-induced vibrations", *Journal of Fluids and Structures*, 19, 389-447.
- [11] Skop R. A. and Balasubramanian S. (1997), "A new twist on an old model for vortex-excited vibrations", *Journal of Fluids and Structures*, 11(4), 395-412.
- [12] Williamson C.H.K., Govardhan R. (2004), "Vortex-induced vibrations", *Annu. Rev. Fluid Mech.*, 36, 413-455.
- [13] Williamson C. H. K., Govardhan R. (2008), "A brief review of recent results in vortex-induced vibrations", *Journal of Wind engineering and industrial Aerodynamics*, 96(6-7), 713-735.
- [14] Yong S, Wang Yong-xue. (2008), "Vortex induced vibrations of finned cylinders", *Journal of Hydrodynamics*, 20(2), 195-201.